4.5.2. Cytotoxicity. Methanol solutions of test compound were put into a 96-well plate and dried completely. Jurkat cells were plated on the sample plate at a density of 2×10^4 cells/well with 100 μL of culture medium. After 3 days cultivation at 37 °C with 5% CO_2, cell density and morphological changes in the cells were observed under a microscope. After observation, 10 μL of MTT solution (5 mg/mL MTT in PBS) was added to the cells and the plate was incubated at 37 °C with 5% CO_2 for 2 h. Then, 50 μL of MTT solvent (0.7 M SDS, 50% DMF, 2.5% 1 M HCl and 2% acetic acid in H_2O) was added to the cells. After 1 h incubation at 37 °C, absorbance at 550 nm was measured.

4.5.3. Antimicrobial assay. Antimicrobial activity was measured using the agar dilution method, according to the method of the Japanese Society of Chemotherapy,[13] with the following strains: *Staphylococcus aureus* ATCC6538P, *Kocuria rhizophila* (*Micrococcus luteus*) ATCC9341, *Bacillus subtilis* ATCC6633, *Mycobacterium smegmatis* ATCC607, *Escherichia coli* NIHJ, *Salmonella typhimurium* KB20, *Pseudomonas aeruginosa* NBRC3080, *Xanthomonas oryzae* KB88, *Bacteroides fragillis* ATCC23745, *Morganella morganii* NBRC3168, *Proteus vulgaris* NBRC3167, *Acholeplasma laidlawii* Bm1 KB175, *Candida albicans* KF1, *Saccharomyces cerevisiae* ATCC9763, *Aspergillus niger* ATCC9642, *Pyricularia oryzae* KF180 and *Mucor racemosus* NBRC4581.

Acknowledgements

We thank Ms. Akiko Nakagawa and Ms. Noriko Sato, School of Pharmacy, Kitasato University for measurement of mass and NMR spectra. This work was supported by The Ministry of Education, Culture, Sports, Science and Technology (MEXT) Grant-in-Aid for Young Scientists (B) 21780115 (to M.M.) and Kitasato University Research Grant for Young Researchers (to M.M.).

References and notes

1. (a) Kita, K.; Nihei, C.; Tomitsuka, E. *Curr. Med. Chem.* **2003**, *10*, 2535–2548; (b) Kita, K.; Shiomi, K.; Ōmura, S. *Trends Parasitol.* **2007**, *23*, 223–229; (c) Masuma, R.; Shiomi, K.; Ōmura, S. In *The Mycota*; Anke, T., Weber, D., Eds.; Springer: Berlin Heidelberg, 2009; Vol. XV, pp 247–271.
2. (a) Ōmura, S.; Miyadera, H.; Ui, H.; Shiomi, K.; Yamaguchi, Y.; Masuma, R.; Nagamitsu, T.; Takano, D.; Sunazuka, T.; Harder, A.; Kölbl, H.; Namikoshi, M.; Miyoshi, H.; Sakamoto, K.; Kita, K. *PNAS* **2001**, *98*, 60–62; (b) Ui, H.; Shiomi, K.; Yamaguchi, Y.; Masuma, R.; Nagamitsu, T.; Takano, D.; Sunazuka, T.; Namikoshi, M.; Ōmura, S. *J. Antibiot.* **2001**, *54*, 234–238.
3. Miyadera, H.; Shiomi, K.; Ui, H.; Yamaguchi, Y.; Masuma, R.; Tomoda, H.; Miyoshi, H.; Osanai, A.; Kita, K.; Ōmura, S. *PNAS* **2003**, *100*, 473–477.
4. Ui, H.; Shiomi, K.; Suzuki, H.; Hatano, H.; Morimoto, H.; Yamaguchi, Y.; Masuma, R.; Sunazuka, T.; Shimamura, H.; Sakamoto, K.; Kita, K.; Miyoshi, H.; Tomoda, H.; Ōmura, S. *J. Antibiot.* **2006**, *59*, 785–790.
5. Ui, H.; Shiomi, K.; Suzuki, H.; Hatano, H.; Morimoto, H.; Yamaguchi, Y.; Masuma, R.; Sakamoto, K.; Kita, K.; Miyoshi, H.; Tomoda, H.; Tanaka, H.; Ōmura, S. *J. Antibiot.* **2006**, *59*, 591–596.
6. (a) de Haan, J. W.; van de Ven, L. J. M. *Tetrahedron Lett.* **1971**, 3965–3968; (b) Crews, P.; Kho-Wiseman, E. *J. Org. Chem.* **1977**, *42*, 2812–2815.
7. (a) Wei, H.; Itoh, T.; Kinoshita, M.; Kotoku, N.; Aoki, S.; Kobayashi, M. *Tetrahedron* **2005**, *61*, 8054–8058; (b) Wei, H.; Itoh, T.; Kotoku, N.; Kobayashi, M. *Heterocycles* **2006**, *68*, 111–123.
8. Lang, G.; Wiese, J.; Schmaljohann, R.; Imhoff, J. F. *Tetrahedron* **2007**, *63*, 11844–11849.
9. Jayasuriya, H.; Guan, Z.; Dombrowski, A. W.; Bills, G. F.; Polishook, J. D.; Jenkins, R. G.; Koch, L.; Crumly, T.; Tamas, T.; Dubois, M.; Misura, A.; Darkin-Rattray, S. J.; Gregory, L.; Singh, S. B. *J. Nat. Prod.* **2007**, *70*, 1364–1367.
10. Dong, Y.; Lin, J.; Lu, X.; Zheng, Z.; Ren, X.; Zhang, H.; He, J.; Yang, J. *Helv. Chim. Acta* **2009**, *92*, 567–574.
11. Prugosene A1 was isolated from molded rice with *Penicillium* sp. FKI-5329 by the same methods as shown in Experimental section. The structure of prugosene A1 was confirmed by the comparison with NMR data and FABMS spectrum.
12. Mosmann, T. *J. Immunol. Methods* **1983**, *65*, 55–63.
13. Nagayama, A.; Yamaguchi, K.; Watanabe, K.; Tanaka, M.; Kobayashi, I.; Nagasawa, Z. *J. Infect. Chemother.* **2008**, *14*, 383–392.
14. Saruta, F.; Kuramochi, T.; Nakamura, K.; Takamiya, S.; Yu, Y.; Aoki, T.; Sekimizu, K.; Kojima, S.; Kita, K. *J. Biol. Chem.* **1995**, *270*, 928–932.

Molecular interaction of the first 3 enzymes of the *de novo* pyrimidine biosynthetic pathway of *Trypanosoma cruzi*

Takeshi Nara[a,*], Muneaki Hashimoto[a], Hiroko Hirawake[a], Chien-Wei Liao[a,b], Yoshihisa Fukai[a], Shigeo Suzuki[a], Akiko Tsubouchi[a], Jorge Morales[a], Shinzaburo Takamiya[a], Tsutomu Fujimura[b], Hikari Taka[b], Reiko Mineki[b], Chia-Kwung Fan[c], Daniel Ken Inaoka[d], Masayuki Inoue[e], Akiko Tanaka[f], Shigeharu Harada[g], Kiyoshi Kita[d], Takashi Aoki[a]

[a]Department of Molecular and Cellular Parasitology, Juntendo University Graduate School of Medicine, 2-1-1 Hongo, Bunkyo-ku, Tokyo 113-8421, Japan

[b]Division of Proteomics and Biomolecular Science, Biomedical Research Center, Juntendo University Graduate School of Medicine, 2-1-1 Hongo, Bunkyo-ku, Tokyo 113-8421, Japan

[c]Department of Parasitology, Taipei Medical University, 250 Wu-Xing Street, Taipei 110, Taiwan R.O.C.

[d]Department of Biomedical Chemistry, Graduate School of Medicine, The University of Tokyo, 7-3-1 Hongo, Bunkyo-ku, Tokyo 113-0033, Japan

[e]Graduate School of Pharmaceutical Sciences, The University of Tokyo, 7-3-1 Hongo, Bunkyo-ku, Tokyo 113-0033, Japan

[f]Systems and Structural Biology Center, RIKEN, Tsurumi, Yokohama 230-0045, Japan

[g]Department of Applied Biology, Graduate School of Science and Technology, Kyoto Institute of Technology, Sakyo-ku, Kyoto 606-8585, Japan

*Corresponding author:

Department of Molecular and Cellular Parasitology, Juntendo University Graduate School of Medicine, 2-1-1 Hongo, Bunkyo-ku, Tokyo 113-8421, Japan

Tel: +81-3-5802-1043; Fax: +81-3-5800-0476; E-mail: tnara@juntendo.ac.jp

Footnote 1:

Abbreviations: CPSII, carbamoyl-phosphate synthetase II; ATC, aspartate transcarbamoylase; DHO, dihydroorotase; CAD, CPSII-DHO-ATC fusion enzyme; UMP, uridine 5′-monophosphate; SBDD, structure-based drug design

ABSTRACT

The first 3 reaction steps of the *de novo* pyrimidine biosynthetic pathway are catalyzed by carbamoyl-phosphate synthetase II (CPSII), aspartate transcarbamoylase (ATC), and dihydroorotase (DHO), respectively. In eukaryotes, these enzymes are structurally classified into 2 types: (1) a CPSII-DHO-ATC fusion enzyme (CAD) found in animals, fungi, and amoebozoa, and (2) stand-alone enzymes found in plants and the protist groups. In the present study, we demonstrate direct intermolecular interactions between CPSII, ATC, and DHO of the parasitic protist *Trypanosoma cruzi,* which is the causative agent of Chagas disease. The 3 enzymes were expressed in a bacterial expression system and their interactions were examined. Immunoprecipitation using an antibody specific for each enzyme coupled with western blotting-based detection using antibodies for the counterpart enzymes showed co-precipitation of all 3 enzymes. From an evolutionary viewpoint, the formation of a functional tri-enzyme complex may have preceded—and led to—gene fusion to produce the CAD protein. This is the first report to demonstrate the structural basis of these 3 enzymes as a model of CAD. Moreover, in conjunction with the essentiality of *de novo* pyrimidine biosynthesis in the parasite, our findings provide a rationale for new strategies for developing drugs for Chagas disease, which target the intermolecular interactions of these 3 enzymes.

Keywords: *de novo* pyrimidine biosynthetic pathway; carbamoyl phosphate synthetase II; aspartate transcarbamoylase; dihydroorotase; *Trypanosoma cruzi*

INTRODUCTION

The *de novo* pyrimidine biosynthetic pathway consists of 6 enzymes required for the production of uridine 5′-monophosphate (UMP). In eukaryotes, the primary structure of the first 3 enzymes in this pathway, carbamoyl-phosphate synthetase II (CPSII; EC 6.3.5.5), aspartate transcarbamoylase (ATC; EC 2.1.3.2), and dihydroorotase (DHO; EC 3.5.2.3), is divided into 2 types [1]. A fusion enzyme of CPSII-DHO-ATC (CAD) is found in animals, fungi, amoebozoa, and also in the red alga *Cyanidioschyzon merolae* [2,3]. In contrast, the individual, stand-alone enzymes are common among the remaining eukaryotic groups.

Gene fusion results in the formation of multifunctional proteins and is one of the major driving forces in protein evolution. CAD has arisen from an ancient fusion between its monofunctional counterparts, which may result in enhanced channeling of substrates through each catalytic site [4]. From a biochemical viewpoint, it is assumed that formation of a complex of the enzymes preceded gene fusion and contributed to the precise order and topology of the domains within the fused enzyme. Moreover, ATC and DHO constitute an enzyme complex in a subset of bacteria [5,6], suggesting possible complex formation between eukaryotic ATC and DHO. Thus, it is highly likely that a tri-enzyme complex of stand-alone CPSII, ATC, and DHO preceded—and eventually led to—gene fusion to produce the multifunctional CAD protein, which may share tertiary structural similarity.

We have previously showed that CPSII, ATC, and DHO are stand-alone enzymes in the parasitic protist *Trypanosoma cruzi*, which is the causative agent of Chagas disease, an endemic disease in the Latin American countries [7,8]. All 5 genes for the 6 pyrimidine biosynthetic enzymes cluster within trypanosomatid genomes in the following order: *CPSII, DHO, OMPDC-OPRT* (fused gene comprising

the sixth orotidine-5′-monophosphate decarboxylase and the fifth orotate phosphoribosyltransferase enzymes), *DHOD* (the fourth dihydroorotate dehydrogenase enzyme), and *ATC*. Thus, the gene order of *CPSII, DHO*, and *ATC* in trypanosomatid genomes is consistent with the domain order within CAD [7]. Thus, these findings allowed us to investigate the possibility of complex formation between *T. cruzi* CPSII, ATC, and DHO.

From a clinical viewpoint, *de novo* pyrimidine biosynthesis represents a promising drug target, in particular, against Chagas disease and other trypanosomatid diseases such as sleeping sickness and leishmaniasis caused by *T. brucei gambiense/rhodesiense* and *Leishmania* spp., respectively. These trypanosomatid diseases are termed "neglected tropical diseases," and urgently require effective chemotherapeutics with low toxicity [9,10]. Very recently, we demonstrated the importance of CPSII for the growth of *T. cruzi* in the cytoplasm of the mammalian host cells [11]. Therefore, the 3 enzymes and their complex, if present, represent potential targets of chemotherapy for trypanosomatid diseases.

In the present study, we used recombinant enzymes to examine whether CPSII, ATC, and DHO form a tertiary complex. As a result, we demonstrated that these 3 enzymes interact with each other, suggesting that the multifunctional CAD fusion enzyme was preceded by complex formation between CPSII, ATC, and DHO, possibly mimicking their tertiary structures. Thus, our findings provide important insights into the structural interpretation of evolution of enzymes as well as into the new strategic approaches for the development of drugs against Chagas disease.

MATERIALS and METHODS

Plasmid construction

The open reading frames (ORFs) for the *Trypanosoma cruzi CPSII* (GenBank ID: AB005063), *ATC* (GenBank ID: AB074139), and *DHO* (GenBank ID: AB010284) genes were subcloned into expression vectors, pET52b (ampicillin-resistant; Novagen, Merck Ltd., Tokyo, Japan), pET28a (kanamycin-resistant; Novagen), and pT-GroE (chloramphenicol-resistant) [12]. Prior to cloning, pET52b was modified using the Gateway® Vector Conversion System (Invitrogen, Life Technologies Japan Ltd., Tokyo, Japan) by ligating a reading frame cassette A (RfA) to the *Sma*I site present in pET52b. The resulting plasmid was designated pET52bGW. For cloning of CPSII, the CPSII ORF was amplified using primers (sense, 5′-CACCATGTTTGGGGAAAAAGTGAA-3′; antisense, 5′-TCAACACTGAACGTCGCTGAAGGAGC-3′) and the phage clone carrying *CPSII*, subcloned into the pENTR vector (Invitrogen), and subsequently cloned into pET52bGW via the Clonase® reaction (Invitrogen). For expression of ATC, a pET14b plasmid carrying *ATC* [13] was digested with *Bam*HI and the resulting DNA fragment was cloned into pET28a. For expression of DHO, the ORF was amplified by PCR using a primer set (sense, 5′-CACCATGACGCGGGTGGAACTGCC-3′ and antisense, 5′-CTAAATAGCCTTACCAACAAG-3′), subcloned into pENTR, and finally cloned into pET52bGW. Alternatively, the ORF of DHO was amplified using primers (sense, 5′-GCGAATTCCATATGACGCG-3′; antisense, 5′-GCGGATCCTAAATAGCC-3′) and the phage clone carrying *DHO* [7] and subcloned into the pT7 BlueT vector. The *Nde*I/*Bam*HI fragment was further subcloned into *Nde*I/*Bam*HI-treated pT-GroE, in which the *GroESL* gene was cleaved off.

Expression of recombinant enzymes

Recombinant plasmids were introduced into *Escherichia coli* BL21 Star™ (DE3) cells

(Invitrogen), either independently or in combination. The *E. coli* transformants were precultured by overnight incubation at 37°C in Luria–Bertani (LB) medium containing the appropriate antibiotics. Subsequently, a total of 0.8 ml of the bacterial culture was centrifuged for 5 min at 1,500 × *g*, and the cells were further cultured at 37°C in 30 ml of antibiotic-supplemented LB medium until the OD_{600} reached 0.8. Expression was induced at 25°C for 1 h in the presence of 0.4 mM isopropyl-β-D-thiogalactopyranoside. The cells were harvested by centrifugation at 1,500 × *g* for 10 min and suspended in 2 ml of IP buffer (150 mM NaCl, 10 mM Tris-HCl [pH7.4], 1 mM EDTA, 1 mM EGTA, 1% Triton X-100, 1.5% NP-40, 0.2 mM sodium orthovanadate, and 0.2 mM PMSF) supplemented with a protease inhibitor cocktail (Complete Mini, Roche Diagnostics K.K., Tokyo, Japan). After disruption of cells by sonication, the lysate was centrifuged at 15,000 × *g*, 4°C for 10 min. The resulting supernatant containing the soluble enzymes was collected and used for immunoprecipitation experiments.

Antibodies

Rabbit polyclonal IgG was raised against *T. cruzi* CPSII (polypeptide, aa1–17; Sigma-Aldrich, St. Louis, MO) and DHO (polypeptide, aa12–29; BioGate Ltd, Gifu, Japan), and mouse polyclonal antisera was raised against recombinant *T. cruzi* ATC.

Immunoprecipitation

Immunoprecipitation was carried out using the enzyme-specific antibodies and Protein G Magnetic Beads (New England Biolabs, Beverly, MA) under the conditions recommended by the manufacturer. Briefly, 200 μl of bacterial lysate was incubated at 4°C for 1 h with 1.5 μg of purified IgG specific for each enzyme, followed by incubation

with 25 μl of the beads at 4°C for 1 h. The resulting precipitates were recovered magnetically, separated by SDS-PAGE, and transferred to PVDF membranes. The membrane was reacted with enzyme-specific antibodies and visualized using alkaline phosphatase-conjugated secondary antibody and colorimetric substrates.

RESULTS and DISCUSSION

The activities of CPSII, ATC, and DHO enzymes in trypanosomatids have been purified separately by gel chromatography or ammonium sulfate precipitation [14,15], suggesting that the 3 enzymes are not covalently linked, or that weak interactions occur between them. Thus, we aimed to examine the molecular interactions between *T. cruzi* CPSII, ATC, and DHO by using purified enzymes that were independently expressed in a bacterial expression system (Fig. 1). *T. cruzi* ATC was efficiently expressed as a soluble protein and purified to apparent homogeneity, as reported previously [13]. However, individual expression of *T. cruzi* CPSII or DHO was difficult, and these enzymes were mainly expressed as insoluble inclusion bodies. The un-tagged recombinant *T. cruzi* DHO protein appeared to be toxic to *E. coli*, since the transformant colonies were very small (data not shown). This may be due to heterodimerization between bacterial and *T. cruzi* DHO proteins, thereby leading to impaired *de novo* pyrimidine biosynthesis by the bacteria. Furthermore, we also failed to obtain efficient expression of a soluble form of GST-tagged DHO.

Although these results suggest that individually expressed CPSII and DHO were highly unstable in the bacteria, we tried to examine whether the individually expressed enzymes formed a complex, which would stabilize these enzymes. The soluble fractions of each bacterial lysate were mixed, immunoprecipitated using the respective antibodies, and probed by western blot analysis. However, no association

was seen between the individually expressed target proteins.

Therefore, we examined the interactions between the 3 proteins by co-expressing CPSII, ATC, and DHO using pET52b (ampicillin-resistant), pET28a (kanamycin-resistant), and pTGroE (chloramphenicol-resistant) expression vectors, respectively, in order to confer antibiotic selection. Under these conditions, the transformed bacteria grew normally. After induction of expression, the bacterial lysates were immunoprecipitated using either CPSII- or ATC- or DHO-specific antibodies and subjected to western blot analysis. As shown in Fig. 2, all 3 enzymes were co-precipitated by a pull-down assay using antibodies specific to either enzyme (Fig. 2). Namely, immunoprecipitation using the CPSII-specific antibody was accompanied by co-precipitation of both ATC and DHO, and the ATC- or DHO-specific antibodies allowed co-precipitation of CPSII plus DHO or CPSII plus ATC, respectively. Thus, these results clearly indicate the existence of a molecular interaction between CPSII, ATC, and DHO.

Co-precipitation of ATC and DHO in the CPSII-specific precipitate was further confirmed by in-gel digestion coupled with liquid chromatography-tandem mass spectrometry (LC-MS/MS) of the corresponding protein bands separated by SDS-PAGE (Supplementary Fig. S1). The sequence coverage scores for ATC and DHO were 52% and 51%, respectively. In addition, the ATC-specific precipitate was found to contain CPSII and DHO, and CPSII and ATC were detected in the DHO-specific precipitate (Supplementary Table S1). Therefore, these findings indicate complex formation by these non-covalently linked enzymes.

However, co-precipitation of CPSII with ATC and DHO does not necessarily indicate a direct interaction of CPSII with both ATC and DHO; if ATC interacts with DHO, the interaction of CPSII with either ATC or DHO would allow co-precipitation of

all 3 enzymes. Therefore, we further examined the existence of a direct interaction of CPSII with ATC and DHO. CPSII was co-expressed with either ATC or DHO, and precipitated using the CPSII-specific antibody. Western blot analysis of the precipitates showed direct interactions between both CPSII and ATC and between CPSII and DHO (Fig. 3). Similarly, a direct interaction was also observed between ATC and DHO, which is consistent with results for the bacterial enzymes [5]. These findings strongly suggest that tri-enzyme complex formation between CPSII, ATC, and DHO occurs via direct interactions.

Regarding enzyme stability, native CPSII purified from the kinetoplastid *Crithidia fasciculata*—a close relative of trypanosomatids—was very fragile, and its enzyme activity was rapidly lost during cryopreservation, which may have been accompanied by dissociation of its tertiary structure [16]. In the present study, the molecular interactions between CPSII, ATC, and DHO were stable after repeated freezing and thawing. Therefore, it is possible that complex formation stabilizes enzyme conformation.

Recent advances in drug development have highlighted structure-based drug design (SBDD) as a powerful tool. Moreover, inhibitors of enzymes involved in *de novo* pyrimidine biosynthesis have been extensively studied because of the physiological importance of this pathway, particularly in rapidly growing cells such as cancer cells. However, SBDD has not yet been applied to CAD or its individual counterparts because of difficulties in their expression, purification, and crystallization and the resulting lack of structural information.

In the present study, we demonstrated for the first time the existence of a molecular interaction between *T. cruzi* CPSII, ATC, and DHO enzymes. Furthermore, the efficient expression of these proteins may aid structural analyses and the

elucidation of a model of CAD, thereby leading to SBDD. Indeed, phylogenetic analysis has revealed that the trypanosomatid CPSII and ATC enzymes share common evolutionary origins with the corresponding domains in animal CAD [1].

Moreover, we recently identified the crystal structure of *T. cruzi* ATC [13]. This is the first crystallization of any of the 3 enzymes, including CAD proteins in eukaryotes. Therefore, our findings provide insight into SBDD targeted against trypanosomiasis, particularly aimed at inhibiting intermolecular interactions of the tri-enzymes. Although the phylogenetic relationship between *T. cruzi* DHO and the DHO domain of CAD remains unclarified, it is highly likely that the functional tri-enzyme complex of CPSII, ATC, and DHO occurred in the ancestral eukaryotes, thereby leading to the formation of CAD via fusion of the 3 genes.

Since the *de novo* pyrimidine biosynthetic pathway is a potential primary target of chemotherapy [17,18], our findings may accelerate strategic approaches against trypanosomatid diseases based on SBDD that target the intermolecular interactions of the first 3 enzymes. Further analyses, including crystallography, are necessary to understand the molecular basis of the tri-enzyme complex.

ACKNOWLEDGEMENTS

This work was supported in part by grants-in-aid for the Targeted Proteins Research Program (TPRP), by scientific research No. 19590436 (to T. Nara) and by the Foundation of Strategic Research Projects in Private Universities (S0991013; to T. Nara) from the Ministry of Education, Culture, Sport, Science, and Technology, Japan (MEXT).

REFERENCES

[1] T. Nara, T. Hashimoto, T. Aoki, Evolutionary implications of the mosaic pyrimidine-biosynthetic pathway in eukaryotes. Gene 257 (2000) 209–222.

[2] M. Matsuzaki, O. Misumi, I.T. Shin, et al., Genome sequence of the ultrasmall unicellular red alga *Cyanidioschyzon merolae* 10D. Nature 428 (2004) 653–657.

[3] A. Stechmann, T. Cavalier-Smith, The root of the eukaryote tree pinpointed. Curr. Biol. 13 (2003) R665–666.

[4] E.A. Carrey, The shape of CAD. Paths to Pyrimidines 3 (1995) 68–72.

[5] P. Zhang, P.D. Martin, C. Purcarea, et al., Dihydroorotase from the hyperthermophile *Aquifex aeolicus* is activated by stoichiometric association with aspartate transcarbamoylase and forms a one-pot reactor for pyrimidine biosynthesis. Biochemistry 48 (2009) 766–778.

[6] M.J. Schurr, J.F. Vickrey, A.P. Kumar, et al., Aspartate transcarbamoylase genes of *Pseudomonas putida*: requirement for an inactive dihydroorotase for assembly into the dodecameric holoenzyme. J. Bacteriol. 177 (1995) 1751–1759.

[7] G. Gao, T. Nara, J. Nakajima-Shimada, et al., Novel organization and sequences of five genes encoding all six enzymes for de novo pyrimidine biosynthesis in *Trypanosoma cruzi*. J. Mol. Biol. 285 (1999) 149–161.

[8] T. Nara, G. Gao, H. Yamasaki, et al., Carbamoyl-phosphate synthetase II in kinetoplastids. Biochim. Biophys. Acta 1387 (1998) 462–468.

[9] R. Docampo, Recent developments in the chemotherapy of Chagas disease. Curr. Pharm. Des. 7 (2001) 1157–1164.

[10] J.A. Urbina, Chemotherapy of Chagas disease. Curr. Pharm. Des. 8 (2002)

287–295.

[11] M. Hashimoto, J. Morales, Y. Fukai, et al., Critical importance of the de novo pyrimidine biosynthesis pathway for *Trypanosoma cruzi* growth in the mammalian host cell cytoplasm. Biochem. Biophys. Res. Commun. in press.

[12] T. Yasukawa, C. Kanei-Ishii, T. Maekawa, et al., Increase of solubility of foreign proteins in *Escherichia coli* by coproduction of the bacterial thioredoxin. J. Biol. Chem. 270 (1995) 25328–25331.

[13] K. Matoba, T. Nara, T. Aoki, et al., Crystallization and preliminary X-ray analysis of aspartate transcarbamoylase from the parasitic protist *Trypanosoma cruzi*. Acta Crystallogr. Sect. F Struct. Biol. Cryst. Commun. 65 (2009) 933–936.

[14] T. Aoki, H. Oya, Kinetic properties of carbamoyl-phosphate synthetase II (glutamine-hydrolyzing) in the parasitic protozoan *Crithidia fasciculata* and separation of the enzyme from aspartate carbamoyltransferase. Comp. Biochem. Physiol. B 87 (1987) 143–150.

[15] S. Tampitag, W.J. O'Sullivan, Enzymes of pyrimidine biosynthesis in *Crithidia luciliae*. Mol. Biochem. Parasitol. 19 (1986) 125–134.

[16] T. Aoki, H. Oya, Regulatory properties of carbamoyl-phosphate synthetase II from the parasitic protozoan *Crithidia fasciculata*. Comp. Biochem. Physiol. B 87 (1987) 655–658.

[17] J.A. Urbina, R. Docampo, Specific chemotherapy of Chagas disease: controversies and advances. Trends Parasitol. 19 (2003) 495–501.

[18] T. Annoura, T. Nara, T. Makiuchi, et al., The origin of dihydroorotate dehydrogenase genes of kinetoplastids, with special reference to their biological significance and adaptation to anaerobic, parasitic conditions. J. Mol. Evol. 60 (2005) 113–127.

FIGURE LEGENDS

Figure 1. Expression of the first 3 enzymes of the *Trypanosoma cruzi de novo* pyrimidine biosynthetic pathway in a bacterial expression system

Carbamoyl-phosphate synthetase II (CPSII), aspartate transcarbamoylase (ATC), and dihydroorotase (DHO) were independently expressed in *E. coli* BL21 (DE3) Star cells, separated by SDS-PAGE, and stained with Coomasie Brilliant Blue. Recombinant CPSII and DHO were expressed mostly in the insoluble fractions (P), whereas ATC was expressed in both soluble (S) and insoluble fractions. The arrowheads indicate the respective protein bands.

Figure 2. Immunoprecipitation analysis of *E. coli* lysates co-expressing CPSII, ATC, and DHO

Western blot analysis was performed using antibodies specific to CPSII (panel A), ATC (panel B), and DHO (panel C). The *E. coli* lysates (lane 2) were immunoprecipitated using antibodies specific to CPSII (lane 3), ATC (lane 4), and DHO (lane 5), and examined by western blotting. Precipitates using protein G beads in the absence of antibodies were loaded as a negative control (lane 6). An arrowhead indicates the respective target band. Lane 1, molecular weight marker.

Figure 3. Detection of the direct interactions between CPSII, ATC, and DHO

In panel A, the bacterial lysates expressing CPSII together with ATC (lane 1) or DHO (lane 2) were immunoprecipitated using antibodies specific to the respective enzyme and probed using the CPSII-specific antibody (left). Alternatively, the bacterial extracts (E) expressing CPSII plus ATC or CPSII plus DHO were immunoprecipitated using the

CPSII-specific antibody (S) and reacted with the antibody for ATC (middle) or DHO (right). In panel B, the bacterial extracts expressing ATC and DHO were immunoprecipitated using the antibody (S) for DHO (left) or ATC (right) and probed using the antibody for the counterpart enzymes. The immunoprecipitates in the absence of antibody (N) were loaded as a negative control. An arrowhead indicates the respective target band.

Figure 1

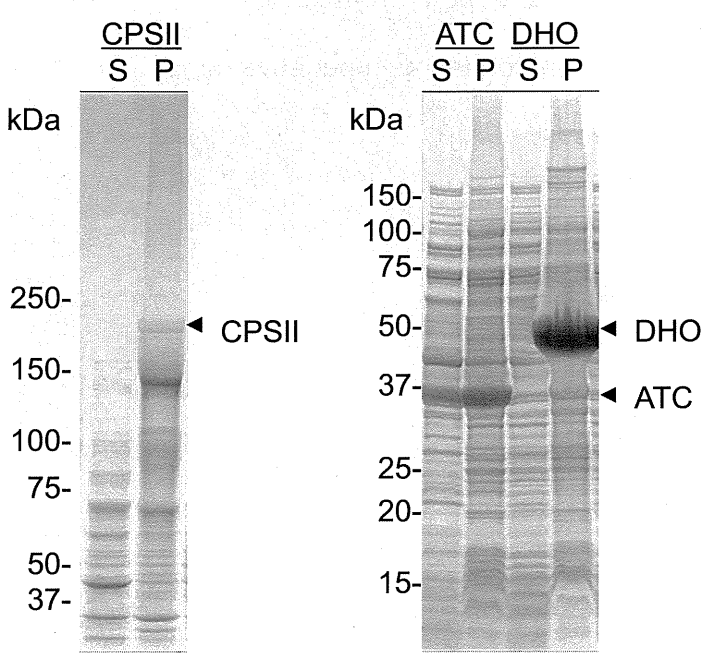
CPSII
S P
kDa
250-
150-
100-
75-
50-
37-
CPSII
ATC DHO
S P S P
kDa
150-
100-
75-
50-
37-
25-
20-
15-
DHO
ATC

Figure 2

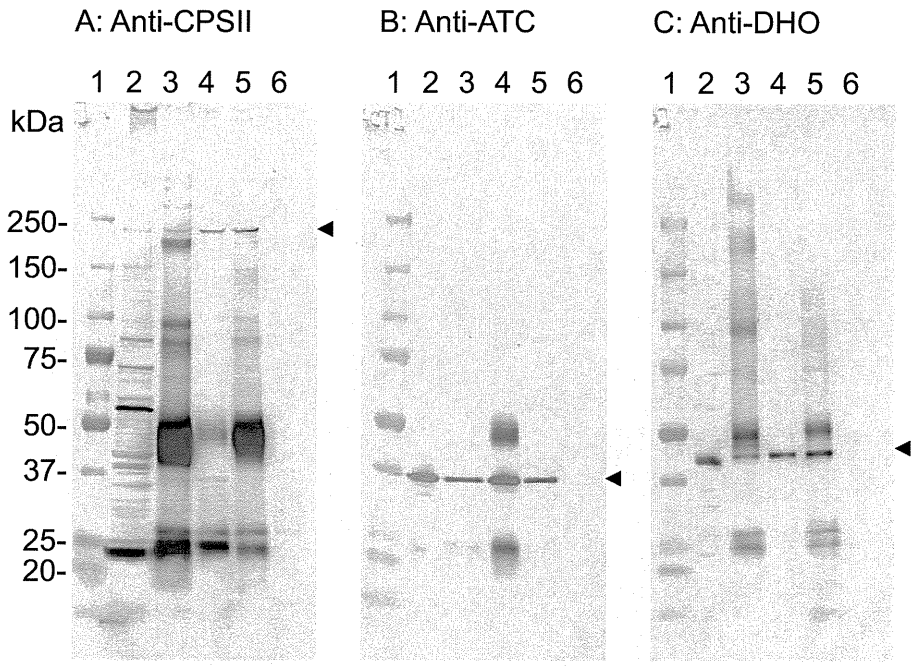
A: Anti-CPSII
B: Anti-ATC
C: Anti-DHO
1 2 3 4 5 6
1 2 3 4 5 6
1 2 3 4 5 6
kDa
250-
150-
100-
75-
50-
37-
25-
20-

Figure 3

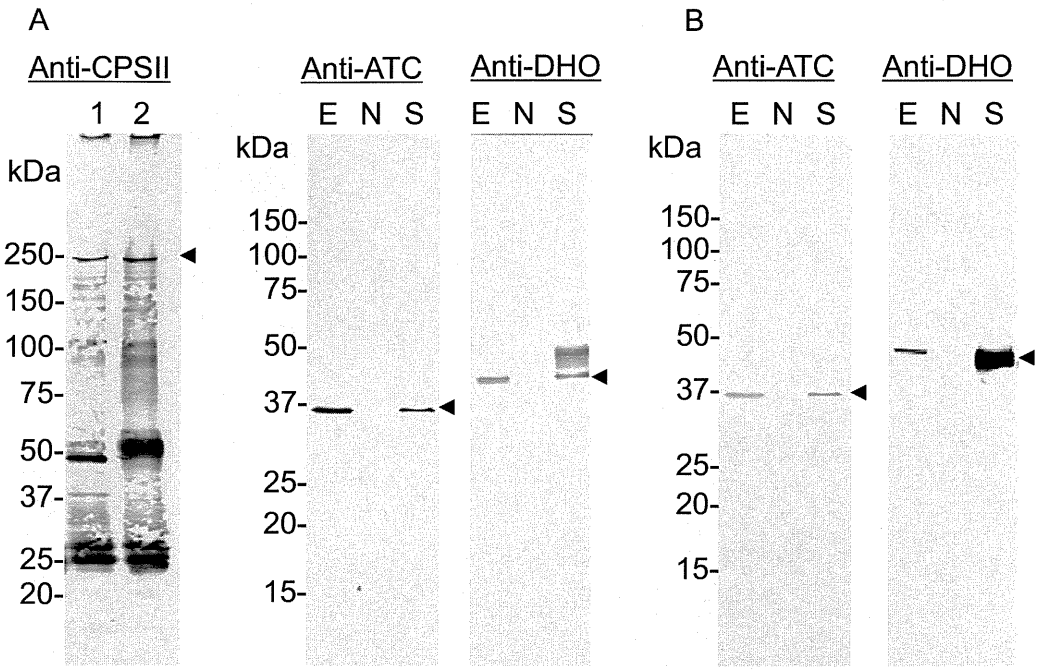
A
Anti-CPSII
1 2
kDa
250-
150-
100-
75-
50-
37-
25-
20-
Anti-ATC
E N S
kDa
150-
100-
75-
50-
37-
25-
20-
15-
Anti-DHO
E N S
B
Anti-ATC
E N S
kDa
150-
100-
75-
50-
37-
25-
20-
15-
Anti-DHO
E N S

Electronic Supplementary Material (online publication only)
Click here to download Electronic Supplementary Material (online publication only): 111228_CAD_interaction_Supplementary.d